Intraparticle Diffusion in the Catalytic Combustion of Methane, Ethane, and Propane

N. T. Thomas and Ken Nobe

University of California, Los Angeles, Calif. 90024

■ The effects of pore diffusion in the catalytic combustion of methane, ethane, and propane have been investigated with CuO-Al$_2$O$_3$ catalyst pellets of two different sizes. Analysis of the experimental data indicates that pore diffusion effects were negligible for the smaller pellets, but not for the larger pellets. Good agreement between the calculated and experimental data of the larger pellets was obtained by considering both surface diffusion and gas-phase pore diffusion.

I n a continuation of investigations on the catalytic elimination of air pollutants from hydrocarbon-consuming combustion processes, the catalytic oxidation reactions of methane, ethane, and propane on CuO-Al$_2$O$_3$ reported previously (Accomazzo and Nobe, 1965) were re-examined to determine the extent of pore diffusion effects. In the correlations of his experimental data, Accomazzo attributed the deviations between experiment and the calculations to external and internal diffusion. The effects of external diffusion were easily determined by calculations and shown to be of relatively minor importance. The discrepancy between the experimental and calculated (including the effects of external diffusion) data was surmised to be due to intraparticle diffusion. The purpose of this work was to investigate in detail the role of pore diffusion in the combustion of methane, ethane, and propane on CuO-Al$_2$O$_3$. The CuO-Al$_2$O$_3$ catalysts prepared by Accomazzo (1965) and aged in air for over 3 years were used. The full-sized cylindrical pellets were 0.3 × 0.25 cm.; half-sized pellets were the full-sized ones cut in half. In theory, pore diffusion effects decrease with decrease in the catalyst size.

Thiele (1939) treated the diffusion of reactants in an ideal catalyst pore mathematically. He introduced the concept of the effectiveness factor, which is defined as the ratio of actual reaction rate to the rate that would be observed if all of the catalyst surface were at the same conditions as the external surface. The major part of the surface area of a highly porous catalyst is, of course, in its interior.

Reviews on pore diffusion effects and equations for the effectiveness factors of different geometries are given by Satterfield and Sherwood (1963), Weisz and Prater (1954), and Wheeler (1951).

The effectiveness factor, η, of first-order reactions on cylindrical pellets has been determined by Aris (1957) as

$$\eta = 1 - \frac{32}{\pi^2} \sum_{m=1}^{\infty} \sum_{n=0}^{\infty} \frac{1}{(2n+1)^2 j_m{}^2} \times$$
$$\frac{\lambda^2 R_c{}^2}{\lambda^2 R_c{}^2 + j_m{}^2 + \frac{\pi^2 R_c{}^2}{L_c{}^2}(2n+1)^2} \quad (1)$$

where $\lambda^2 = \dfrac{k_v}{D_e} = \dfrac{k_p RT}{V_p D_e}$.

The effective diffusivity, D_e, can be determined experimentally. However, calculation methods approximate this parameter. The effective diffusivity can be determined from the diffusivity ratio, ratio of the effective diffusivity of the gas per unit volume of the catalyst to the diffusivity (diffusion coefficient) of the gas per unit volume of the free space. For the latter, the ordinary bulk diffusion coefficient can be used if the pore size is greater than 10,000 A. or the Knudsen coefficient if it is less than 1000 A. under normal conditions of temperature and pressure. For intermediate pore sizes, there is a transition from Knudsen to bulk diffusion and the diffusion coefficient can be estimated by the Bosanquet interpolation formula (Pollard and Present, 1948),

$$\frac{1}{D} = \frac{1}{D_{bd}} + \frac{1}{D_k} \quad (2)$$

Weisz and Schwartz (1962) give an empirical equation for the diffusivity ratio, $\dfrac{D_e}{D} = \dfrac{\epsilon^2}{\sqrt{3}}$, which provides a method of approximating D_e. However, the effective diffusivity calculated by this method assumes that diffusion in the pores proceeds only by gas-phase diffusion. Smith and his coworkers (Krasuk and Smith, 1965; Rivarola and Smith, 1964) have shown that surface diffusion may also contribute to the mass transfer in the pores.

Experimental

The CuO-Al$_2$O$_3$ catalyst prepared by Accomazzo (1965) was aged in air for over 3 years. Cupric nitrate and alumina were mixed in distilled water and the mixture was heated. Then, copper hydroxide was precipitated from the solution by the addition of potassium hydroxide. The precipitate was

filtered, washed, pressed into molds, and then heated in an oven to decompose the copper hydroxide to cupric oxide.

BET surface areas of the catalysts were measured by adsorption of nitrogen gas at liquid nitrogen temperatures. Pore volume was determined by the water injection method. The physical properties of the catalyst are listed in Table I.

A schematic diagram of the equipment and apparatus is shown in Figure 1. The reactor was constructed of Vycor tubing, 19-mm. i.d., with a thermocouple well placed along the axis of the reactor tube. The annulus of the reactor was packed with ceramic beads to a depth of 50 cm. with 16 grams of the catalyst placed on top of the beads. The reactor was enclosed in an electric furnace consisting of two sections with two variable-resistance controls.

Laboratory air freed of carbon dioxide and water vapor by passage through a molecular sieve bed was metered by a calibrated flowmeter. Methane, ethane, and propane of Matheson C.P. grade (minimum purity, 99.5%) were used. The flow rate of hydrocarbons was controlled by a pressure regulator and precision needle valve and determined with a 10-ml. soap bubble buret. The initial concentration was determined by the ratio of the flow rates of hydrocarbon to air. The hydrocarbon and air were completely mixed in the mixing chamber.

In order to attain as nearly as possible isothermal conditions within the reactor, the axial temperature gradient across the catalyst bed was minimized by carefully controlling the variable resistances. The temperature profile in the bed was determined by seven iron-constantan thermocouples and continuously monitored with a Brown 0° to 1200° F. multipoint recorder. The maximum temperature difference of 10° C. across the bed (bed temperatures ~500° C.) was observed at the higher concentration and at high per cent conversion during methane oxidation. However, for all hydrocarbons at intermediate and low per cent conversion, the temperature gradient was 2° C. or less.

After the oxidation of methane, ethane, and propane with the full-size pellets, the catalyst was removed from the reactor and the pellets were cut in half with a razor. The catalyst was then placed in the reactor again. Some borosilicate glass distillation helices were placed over the catalyst bed to minimize fluidization.

The hydrocarbon-air mixture was sampled at the entrance and the exit of the catalyst bed with the hydrocarbon concentration in the exit stream continuously analyzed until steady state was attained. Then, the concentration of the hydrocarbon in outlet stream was recorded, and the inlet concentration determined. The hydrocarbon concentrations in the experiments with the full-size pellets were measured with a Carad flame ionization analyzer and detector, and in the case of half-size pellets, with a Beckman flame ionization detector, Model 108. The instruments were zeroed with nitrogen and calibrated every day with a known concentration of the hydrocarbon used. The output of the analyzer was connected to a Leeds and Northrup recorder to indicate when steady-state condition was achieved.

Table I. Physical Properties of CuO-Al₂O₃ Catalyst

Diameter, mm.	3.0
Length, mm.	2.5
Weight per pellet, g.	0.028
Surface area, sq. m./g.	96
Pore volume, ml./g.	0.415
Mean pore radius, A.	86
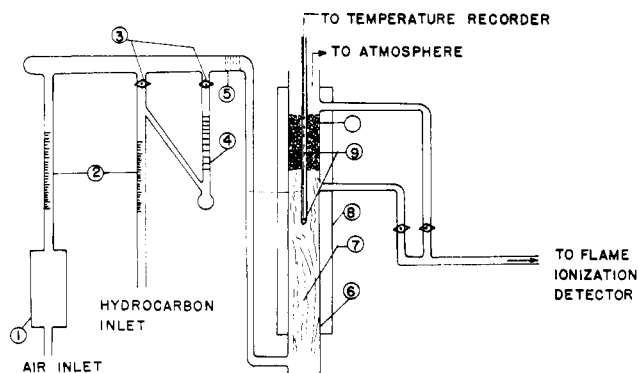
Figure 1. Apparatus

1. Molecular sieve trap	6. Vycor tubing
2. Rotameters	7. Ceramic packing
3. Teflon stopcocks	8. Furnace
4. Soap bubble buret	9. Thermocouple well
5. Mixing disks	10. Catalyst bed

The catalyst was activated before the experiment by passing air at 600° C. for 48 hours through the bed. This procedure was repeated with the half-size pellets.

Results and Discussion

Total gas flow rates of 525 and 275 liters per hour at normal temperatures and pressures were used for each hydrocarbon. Typical experimental data on methane, ethane, and propane combustion with full-size pellets are shown in Figure 2. Conversion of hydrocarbons increased with increase in temperature and with decrease in the flow rate. Methane was the most difficult to oxidize of the three hydrocarbons. Typical data for the combustion of hydrocarbons with half-size pellets of the catalyst are given in Table II. Conversion of hydrocarbons with half-size pellets was always greater than with full-size, as expected. The temperatures required for 50% conversion with full-size pellets at a flow rate of 275 liters per hour were 442°, 377°, and 340° C. for methane, ethane, and propane, respectively; with half-size pellets, 404°, 349°, and 326° C. for methane, ethane, and propane, respectively.

The rate expression $r = k_p p_H^n$ was used to correlate all the data, where p_H is the partial pressure of the hydrocarbon. The experimental data on methane, ethane, and propane combustion with full-size and half-size pellets of copper oxide

Figure 2. Experimental and calculated data for combustion of methane, ethane, and propane on full-sized $CuO-Al_2O_3$ pellets

○ ● Methane
△ Ethane
□ Propane
Points represent experimental data
Continuous lines represent calculated data

Open points. 275 liters per hour
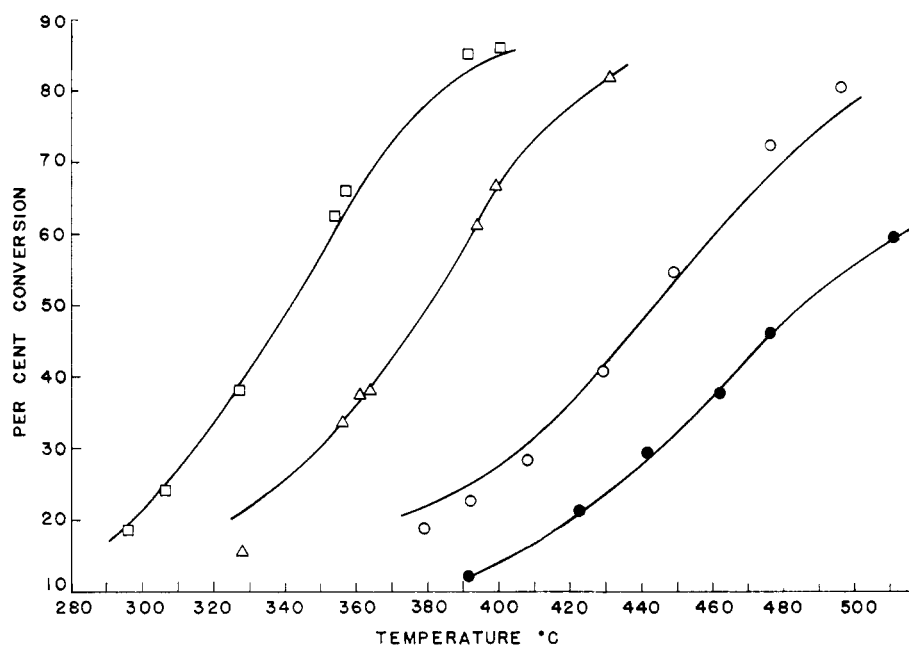
Closed points. 525 liters per hour

Table II. Catalytic Combustion of Hydrocarbons on Half-Size Pellets

Hydrocarbon	Q, L./Hr.	$P_0 \times 10^6$, Atm.	T, °C.	% Oxidation	Hydrocarbon	Q, L./Hr.	$P_0 \times 10^6$, Atm.	T, °C.	% Oxidation
Methane	275	565	380	34	Ethane	525	740	320	24
		565	390	40			740	340	38
		565	400	47			740	350	45
		565	410	54			740	360	53
		565	420	60			740	370	61
		565	430	67			740	380	68
		565	440	73			740	390	75
		565	450	78			740	400	81
		565	460	83			740	410	87
		565	480	91			740	420	92
		565	490	94					
	525	1030	400	29	Propane	275	665	300	28
		1030	410	33			665	310	35
		1030	420	39			665	320	44
		1030	430	45			665	330	54
		1030	440	53			665	340	64
		1030	450	60			665	350	73
		1030	460	67			665	360	83
		1030	480	78			665	370	90
		1030	490	84			665	380	95
							665	390	98
Ethane	275	830	330	35		525	770	300	15
		830	340	44			770	310	20
		830	350	53			770	320	26
		830	360	62			770	330	35
		830	370	72			770	340	44
		830	380	81			770	350	54
		830	390	88			770	360	64
		830	400	93			770	370	73
		830	410	95			770	380	80

were initially examined neglecting diffusion effects in order to obtain a first approximation of the apparent reaction order and other kinetic parameters.

The reduction of the data for the combustion of methane, ethane, and propane with full-size and half-size pellets assuming a first-order reaction with respect to the hydrocarbon concentration is shown in the Arrhenius plots in Figures 3 and 4. The Arrhenius curves were linear for the half-size and

nonlinear for the full-size pellets. Comparison of the difference between the degree of oxidation on the full-size and half-size pellets at a specific temperature shows that this difference decreases as the temperature decreases and in the following order: methane > ethane > propane. In addition, the half-size pellets were more active than the full-size pellets. These results indicate that pore diffusion effects were negligible for the half-size pellets, but significant for the full-size pellets.
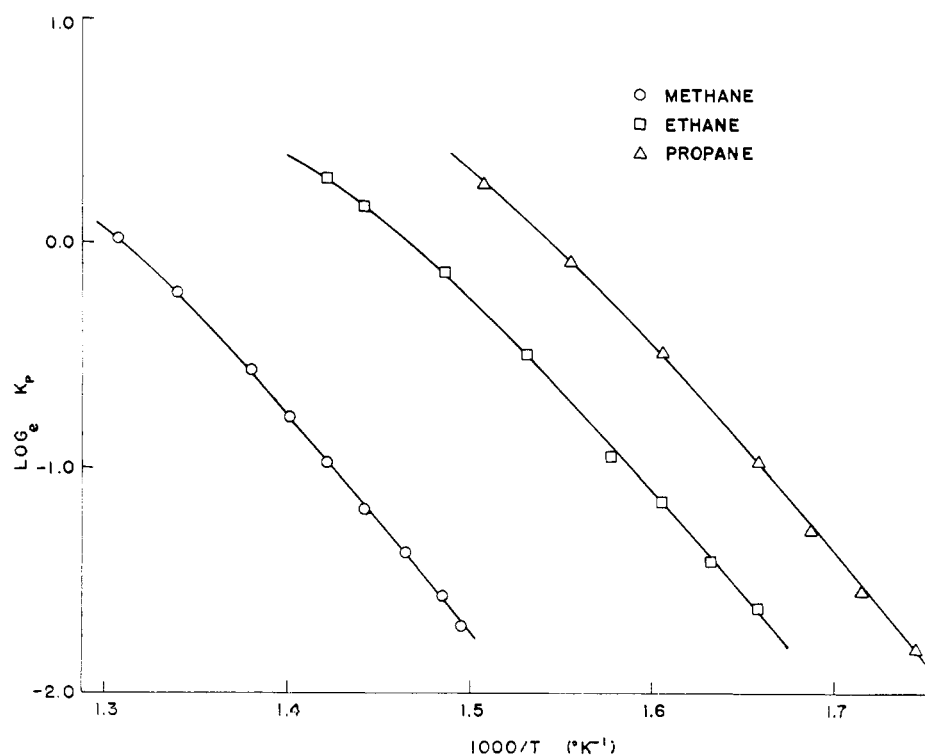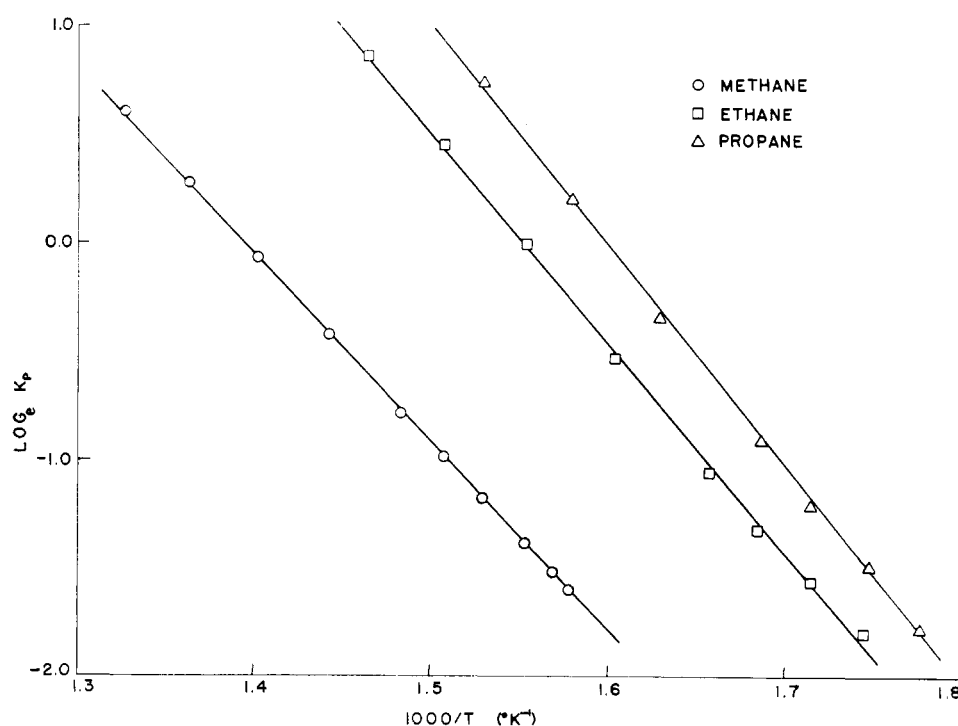
Figure 3. Arrhenius plots for full-size pellets

Figure 4. Arrhenius plots for half-size pellets

The rate equations for the combustion of the hydrocarbons with half-size pellets are

$$r_{CH_4} = 2.99 \times 10^5 e^{\frac{-17820}{RT}} p_{CH_4} \qquad (3)$$

$$r_{C_2H_6} = 8.29 \times 10^6 e^{\frac{-19193}{RT}} p_{C_2H_6} \qquad (4)$$

$$r_{C_3H_8} = 1.73 \times 10^2 e^{\frac{-20682}{RT}} p_{C_3H_8} \qquad (5)$$

where p is hydrocarbon partial pressure in atmospheres and r is the rate in gram moles/hour-atmosphere-gram of catalyst. With the above kinetic parameters obtained with the half-size pellets, the effects of pore diffusion with the full-size pellets were determined.

The effective diffusivity was calculated using the relation

$$\frac{1}{D_e} = \frac{\sqrt{3}}{\epsilon^2}\left(\frac{1}{D_H} + \frac{1}{D_{kH}}\right) \qquad (6)$$

where ϵ is the porosity of the pellets, D_{kH} is the Knudsen diffusion coefficient of the hydrocarbon, and D_H is the ordinary diffusion coefficient of the hydrocarbon in air. The diffusivity ratio, D_e/D, was determined to be 0.26. To take into account the temperature gradient along the bed and the external diffusion effects, the bed was divided into small increments and the design equation in difference form was used, $\frac{\Delta W}{F} = \frac{\Delta X}{r}$.

The temperatures at each end of the increment were measured with thermocouples placed along the bed. The conversion across the increment was calculated by a trial and error method (Caretto, 1965). Computer calculations taking into account the temperature gradient along the bed determined the conversions at the exit of the reactor by considering pore and external diffusion effects, the effect of external diffusion alone, and finally no diffusion effects.

The results showed that the effects of external diffusion were negligible. The detailed calculations of exit conversion considering both pore and external diffusion showed that the experimental conversions were always greater than the calculated values. This observed higher conversion has been attributed to surface diffusion (Krasuk and Smith, 1965).

Krasuk and Smith (1965) considered the calculation of effectiveness factors for cases where surface diffusion was significant. They calculated effectiveness factors from Miller and Kirk's (1962) catalytic dehydration data of ethanol, 1-propanol, and 1-butanol by replacing the normal diffusion

modulus, λL, by $\lambda L\sqrt{\dfrac{1}{1+\phi}}$, where ϕ is the ratio of the sur-

face-to-gas-phase pore diffusion. Calculations showed that ϕ increased with increase in temperature and increase in chain length of the alcohol. Rivarola and Smith (1964) measured the surface diffusion rate of carbon dioxide on alumina and observed that surface diffusion was as substantial as gas-phase pore diffusion for pellets with large surface areas.

Caretto (1966), investigating the catalystic combustion of cyclohexane, cyclohexene, and benzene with a CuO-Al$_2$O$_3$

catalyst, also showed that surface diffusion may contribute to intraparticle diffusion. With Krasuk and Smith's method (1965), Caretto calculated ϕ values of 1.7, 3.2, and 5.1 for benzene, cyclohexene, and cyclohexane, respectively.

Good correlation between experimental and calculated data of this investigation can be obtained by using larger diffusivity ratios than those determined with Equation 6. The diffusivity ratio required for propane (2.3) was larger than those required for methane and ethane, and was independent of temperature between 296° and 406° C. The diffusivity ratios of methane varied from 0.26 to 1.0 from 379° to 511° C., and of ethane varied from 0.26 to 1.1 from 328° to 431° C.

Following Krasuk and Smith (1965), the ratio of surface-to-gas-phase pore diffusion, ϕ, with the diffusivity ratios of methane, ethane, and propane can be determined by the equation

$$\phi = \frac{\sqrt{3}D_e}{D\epsilon^2} - 1 \qquad (7)$$

The ϕ for methane varied from 0 to 2.8 in the temperature range of the experiments. For ethane, ϕ varied from 0 to 3.2, and for propane, ϕ was 7.8 with no variation with temperature observed. The required diffusivity ratios, the corresponding surface diffusion ratios, ϕ, and the effective factors, η, for methane, ethane, and propane combustion at various temperatures are given in Table III.

Figure 2 shows the results of the calculations considering gas-phase pore diffusion and surface diffusion effects for full-

Table III. Pore Diffusion Parameters in the Catalytic Combustion of Hydrocarbons on Full-Sized Pellets

Hydrocarbon	T, °C.	D_e/D	ϕ	η
Methane	397	0.26	0	0.557
	423	0.30	0.15	0.489
	462	0.60	1.30	0.488
	496	1.00	2.83	0.473
	511	1.00	2.83	0.432
Ethane	328	0.26	0	0.540
	356	0.35	0.34	0.462
	361	0.35	0.34	0.441
	364	0.35	0.34	0.428
	394	0.75	1.88	0.432
	431	1.10	3.22	0.367
Propane	296	2.3	7.8	0.917
	327	2.3	7.8	0.817
	343	2.3	7.8	0.747
	354	2.3	7.8	0.695
	385	2.3	7.8	0.506
	406	2.3	7.8	0.463

size pellets. The linearity of the Arrhenius curves in Figure 4 indicated that for the half-size pellets the pore diffusion effects were negligible. According to theory, the effect of pore diffusion should diminish with decrease in pellet size (the internal characteristics of the catalyst being identical). In other words, if pore diffusion effects are significant, decreasing the pellet size of the catalyst should increase the activity per unit mass of catalyst. Experimental results are thus in qualitative agreement with theory. Comparison of the experimental data for the combustion of methane, ethane, and propane on half-size pellets (Table II and Figure 4) and full-size pellets (Figures 2 and 3) indicates that the effect of pore diffusion for the full-size pellets was significant.

Satterfield and Sherwood (1963) show that catalytic activity increases with decrease in the size of the catalyst. Weisz and Prater (1954) reported that the activity of a silica-alumina catalyst for the cracking of cumene increased with decrease in the catalyst size. Caretto (1965) showed the importance of pore diffusion in the combustion of ethylene with copper oxide-alumina catalysts and indicated that the effects of pore diffusion decrease with decrease in the catalyst size, as expected.

Conclusions

Surface diffusion may play a significant role in the pore diffusion effects of methane, ethane, and propane combustion on $CuO-Al_2O_3$. Since the surface diffusion ratio, ϕ, is a measure of the effects of surface diffusion, the results given in Table III show that surface diffusion relative to gas-phase pore diffusion increased with increase in temperature and with the chain length of the hydrocarbon. These results are in accord with the analysis of Miller and Kirk's data (1962) by Krasuk and Smith (1965).

Nomenclature

D = gas phase diffusivity, sq. cm./sec.
D_E = ordinary diffusion coefficient of hydrocarbon in air, sq. cm./sec.
D_e = effective diffusivity in catalyst particle, sq. cm./sec.
D_e/D = diffusivity ratio
D_K = Knudsen diffusion coefficient, sq. cm./sec.
F = initial feed rate of hydrocarbons, moles/sec.

J_o = zeroth order Bessel function of the first kind
j_m = roots of equation $J_o(j_m) = 0$
k_p = rate constant, moles/sec.-g.cat.-atm.^{n}
k_v = rate constant, moles/sec.-ml.cat.-(moles/ml.)
L_e = length of pore
n = reaction order
p_H = partial pressure of hydrocarbon, atm.
p_o = initial partial pressure of hydrocarbon, atm.
Q = flow rate, liters/sec.
r = reaction rate, moles/sec.-g.cat.
R = gas constant
R_c = cylinder radius
T = temperature, ° K.
V_p = pellet volume, ml./g.
W = weight of catalyst, g.
X = conversion of hydrocarbon
ϵ = porosity of catalyst pellet
η = effectiveness factor
λ = diffusion modulus, cm.$^{-1}$
ϕ = ratio of surface diffusion to gas-phase pore diffusion

Literature Cited

Accomazzo, M. A., Nobe, Ken, *Ind. Eng. Chem. Proc. Design Develop.* **4**, 425 (1965).
Aris, R., *Chem. Eng. Sci.* **6**, 262 (1957).
Caretto, L. S., Ph.D. dissertation, University of California, Los Angeles, June 1965.
Caretto, L. S., Nobe, Ken, *Ind. Eng. Chem. Proc. Design. Develop.* **5**, 217 (1966).
Krasuk, J., Smith, J., *Ind. Eng. Chem. Fundamentals* **4**, 102 (1965).
Miller, D. Kirk, R., *A.I.Ch.E.J.* **8**, 183, (1962).
Pollard, W. G., Present, R. D., *Phys. Rev.* **73**, 762 (1948).
Rivarola, J. Smith, J., *Ind. Eng. Chem. Fundamentals* **3**, 308 (1964).
Satterfield, C. N., Sherwood, T. K., "The Role of Diffusion in Catalysis," Addison-Wesley, Reading, Mass., 1963.
Thiele, E., *Ind. Eng. Chem.* **31**, 916 (1939).
Weisz, P., Prater, C., *Advan. Catalysis* **6**, 143 (1954).
Weisz, P., Schwartz, A. J., *Catalysis* **1**, 399 (1962).
Wheeler, A., *Advan. Catalysis* **3**, 249 (1951).